

A method for low-cost, low-impact insect tracking using retroreflective tags

Michael Thomas Smith* Michael Livingstone † Richard Comont ‡

Abstract

1. Current methods for direct tracking of individual bee movement behaviour have several limitations. In particular, the weight and size of some types of electronic tag may limit their use to larger species. Radars and other electronic systems are also often large and very expensive to deploy. A tool is needed that complements these electronic-tag methods. In particular one that is simple to use, low-cost, can have a high spatial resolution and can be used with smaller insects.

2. This paper presents a candidate method that uses retroreflective tags. These are detected using a camera with a global electronic shutter, with which we take photos with and without a flash, the tags can be detected by comparing these two photos. The small retroreflective tags are simple and light-weight, allowing many bees to be tagged at almost no cost and with little effect on their behaviour.

3. We demonstrate this retroreflector-based tracking system (RTS) with a series of simple experiments: Training and validation with a manually positioned tag; Case studies of individual bees; Tracking multiple bees as they forage in a garden; Use of real-time monitoring to allow easy re-observation to enable a simple floral preference experiment; and a very brief experiment with 3D path reconstruction (integrating two devices). We found we could detect bees to a range of about 35m with the current configuration.

4. We envisage the system will be used in future to increase detection rates in mark-re-observation studies; provide 3D flight path analysis; and for automated long-term monitoring. In summary, this novel tracking method has advantages that complement those of electronic-tag tracking which we believe will lead to new applications and areas of research.

Keywords: bee, flight, insect, mark-and-recapture, retroreflector, tagging, tracking, flight path, foraging, floral resources, identification, neuroethology.

*Department of Computer Science, University of Sheffield m.t.smith@sheffield.ac.uk

†Department of Landscape Architecture, University of Sheffield MLivingstone1@sheffield.ac.uk

‡Bumblebee Conservation Trust, richard.comont@bumblebeeconservation.org

26 1 Introduction

27 Tracking individual bees and other insects in the wild can provide ecologists, conservationists and neuroethologists
28 with valuable information, helping them to investigate foraging range and behaviour (Saville et al., 1997), find
29 nests (Kennedy et al., 2018) and even to understanding cognition and learning (Capaldi and Dyer, 1999). A few
30 indirect tracking/density analysis methods exist, including mark/re-observation studies (Dramstad, 1996), genetic
31 microsatellite approaches (Darvill et al., 2004) and pollen analysis (Beil et al., 2008). Direct tracking is also possible
32 for larger species and usually requires some form of electronic tag on the insect, either active or passive, to enable it
33 to be located using (for example) a VHF radio receiver (e.g. Hagen et al., 2011) or harmonic radar (Osborne et al.,
34 1996, 1999; Tsai et al., 2012; Wolf et al., 2014; Riley et al., 1996; Charvat et al., 2003; Capaldi et al., 2000; Tahir
35 and Brooker, 2011), respectively.

36 At the other end of the spatial/temporal scale are high resolution video recordings of bee flight around nests
37 and flowers, which support cognitive research (e.g. Philippides et al., 2013; Linander et al., 2018). However these
38 bee flight trajectories are typically captured over small distances (typically <1m) in indoor, carefully controlled
39 environments (see also for example, Robert et al., 2018), limiting their utility. See Dell et al. (2014) for a wider
40 review of image-based tracking and a discussion of the need for in-the-field individual tracking.

41 Other applications exist that could be explored with improved tracking tools. For example, the ability to follow
42 queens and workers back to early-stage nests (similar to Kennedy et al., 2018). This would support the study of
43 nests and nest site requirements. Tracking methods could also be combined with other experiments, such as the
44 ongoing investigations into the effect of neonicotinoid exposure on navigation (Fischer et al., 2014).

45 In summary, fundamental to our understanding of bee behaviour and ecology is our ability to track and detect
46 individuals as they forage and explore the landscape. Unfortunately, most methods for insect tracking have significant
47 drawbacks: Mark and recapture (for example to estimate forage range) is reportedly often biased by the location of
48 the observers (Schaffer, 1997) and suffers from very low detection rates due to the size of the foraging area involved
49 (Schaffer, 1997, found that fewer than 1% of marked bumblebees were re-detected). Direct human observation
50 of uniquely marked bees has provided considerable evidence regarding factors that support foraging success (e.g.
51 Nunes-Silva et al., 2010).

52 Azimuthally-scanning harmonic radar has been used to track flying insects for over twenty years (e.g. Osborne
53 et al., 1996; Cant et al., 2005; Milanesio et al., 2016)¹ and has a line of sight (due to 3.2cm wavelength) range of
54 several hundred metres (Osborne et al., 1996). The technique's main shortcoming is that the equipment is very
55 large, very expensive² and bespoke, making it inaccessible to most researchers (O'Neal et al., 2004), particularly in
56 low-income countries. Precision typically is of the order of several metres (Cant et al., 2005). The tags are smaller
57 than the active transmitters used in VHF. Osborne et al. (1996); Capaldi et al. (2000); Wolf et al. (2014) were able

¹See Riley (1995) for some of the more technical details of the system's development.

²Porporato (2019, p31) suggest it cost their project €100,000 to construct.

58 to tag and track *Apis mellifera* with 12mg tags, and Chapman et al. (2004) report that 1mg tags have been used to
59 track tsetse flies. Low-power mobile versions (e.g. using the popular Recco Rescue System, <http://www.recco.com/>
60 at about 30cm wavelength) have been used, with range reported as 13m (Lövei et al., 1997), 40m (Langkilde and
61 Alford, 2002), 50m (Roland et al., 1996) or 60m (Psychoudakis et al., 2008).

62 VHF radio transmitters have also been used to track bumblebees (and butterflies) over even larger ranges than
63 harmonic radar (Hagen et al., 2011; Fisher et al., 2020), with the support of a light aircraft. This approach requires
64 a battery powered transmitter to be attached to the bee. The authors find significant effects on bee behaviour
65 ‘suggesting that the current weight of transmitters (200 mg) may still impose significant energetic costs on the
66 insects’(Hagen et al., 2011). The weight of the device makes it impossible to use with many insects. For reference,
67 Connolly (2015) found the median weight of *Bombus terrestris* subsp. *audax* workers was only 251mg.

68 RFID tags have also been used although these typically require the insect to be within 3cm of the sensor
69 (Nunes-Silva et al., 2019). Another recent electronic-tag alternative, with energy harvested from the insect’s wing
70 beats has been developed. This still has a somewhat heavy and complicated payload for the insect to carry
71 (Shearwood et al., 2017), and has a range similar to the method described in this paper. A final interesting result is
72 the use of LIDAR to track untagged bees (Bender et al., 2003) although this requires a very carefully prepared site
73 and doesn’t allow individual targets to be tracked.

74 RFID aside, all the electronic direct-tracking methods require an antenna to be attached to the insect, making
75 it difficult to use with smaller insects, or those which need to access narrow spaces (such as burrowing insects or
76 those which enter sympetalous flowers). See also Mola and Williams (2019) for a review of methods for studying
77 bumblebee movement. We summarise the most common methods in Figure 1.

78 In this paper we describe an alternative method for detecting and tracking insects in the field that doesn’t
79 require an electronic tag. The equipment required is low-cost. Instead of the electronic tag, we tag the insect with a
80 small retroreflective marker and detect it using a camera and flash. The system is a simple to use self-contained
81 device which can be deployed easily in a wide range of landscapes. The simplicity of the tag means many bees can
82 be labelled at almost no cost. The light-weight simple tags mean there is likely to be less impact on bee behaviour.
83 The imaging accuracy can allow, for example, the precise flower being visited to be identified. The range is limited
84 to about 35m line-of-sight, so we don’t envisage it being a complete replacement for harmonic radar and VHF radio
85 tracking, but anticipate it can provide a very useful method in the ecologist’s toolkit. A few example applications
86 include: tracking bees that are potentially too small for electronic tagging, supporting re-observation studies to
87 increase re-observation rates, 3D flight path analysis, and for automated long-term monitoring and tracking. We
88 anticipate further applications to develop as the method matures.

89

90 We describe several experiments using the system: We start by simply tracking a reflector held by a field worker
91 to assess the capabilities of the system and to generate training data for the machine learning classifier. We next

92 describe and discuss case studies of four different bees (in three field sites) and discuss how the system may aid
 93 re-observation. We then tag many different species of wild bee, tracking them as they forage in a garden, using the
 94 data for path reconstruction and to automatically compute time spent on different plants. We use the device to
 95 allow easy reobservation allowing data to be quickly gathered for a simple floral preference experiment. We also
 96 record aspects of foraging behaviour of tagged and untagged bees to assess the effect of the tags (the result are
 97 detailed in the supplementary). We finally briefly consider its use for 3D path reconstruction through the integration
 98 of two devices monitoring the same bee.

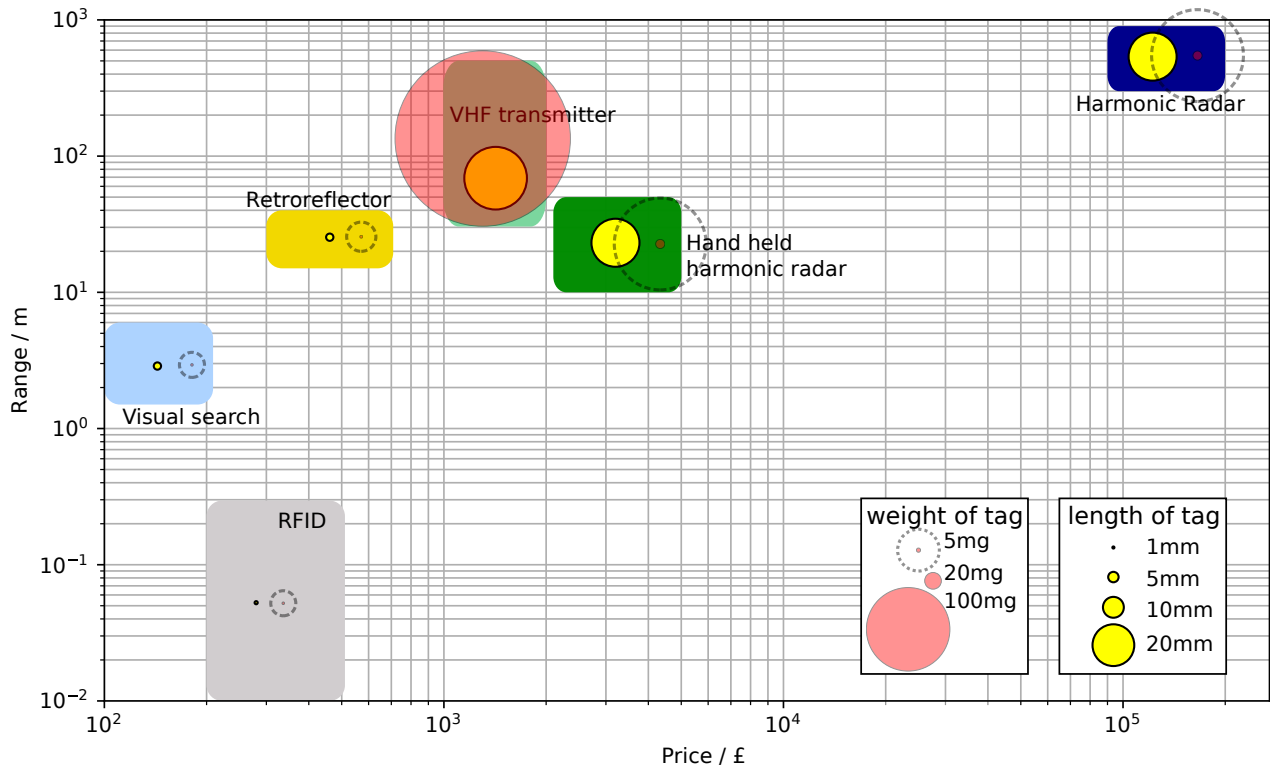


Figure 1: Schematic of six approaches to track individual bumblebees. The x-axis refers to the price of the whole system for tracking. The y-axis indicates the typical maximum range achievable with each system. The yellow circles indicate the length of tag for that method, while the red circles the weight of the tags. Due to the wide range of weights an additional dashed circle (10 times wider) has been added. See text for references regarding weight, size and range².

²Prices were from: Handheld harmonic radar https://www.researchgate.net/post/Can_anybody_provide_information_about_the_equipment_cost_to_assemble_a_harmonic_radar_to_track_insects; Harmonic radar, Porporato (2019, p31); VHF, <https://atstrack.com/animal-class/insects.aspx>; RFID, Bridge et al. (2019). Human visual search range based on standard transect beewalk protocols (Dramstad, 1996; Comont and Miles, 2019).

99 **2 Materials and Methods**

100 **2.1 Overview**

101 The Retroreflector-based Tracking System (RTS) was developed using commercially available components and is
102 simple to construct. The onboard software required is provided as open source modules and as an image for an SD
103 card, allowing researchers to start using the system quickly and easily.

104 Its operation is simple: A camera and flash are mounted on an elevated platform. Pairs of photos are taken,
105 with and without the flash. A retroreflector attached to the bee reflects the flash's light back towards the camera.
106 The non-flash photo is subtracted from the flash photo. A bright dot will remain on the photo after the subtraction,
107 indicating where the retroreflector is. This bright dot can be followed if multiple photo-pairs are taken. Various
108 additional steps, described later, are required to reduce the false positive rate. This algorithm is run in real-time on
109 the system's onboard raspberry pi computer, and the results are both saved internally and made available via a
110 web interface hosted onboard allowing the fieldworker to find the detected bee in real-time (using a mobile phone's
111 browser, for example).

112 **2.2 Bee Capture and Tagging**

113 Over the course of the project we successfully tagged over 100 bees, and find this of similar technical difficulty as
114 tagging in normal reobservation studies. After capture we used cold-induced narcosis to immobilise the bees for
115 tagging (see Supplementary for more details).

116 We use a retroreflector with fabric substrate (from a hi-vis jacket) and cut it approximately to $8 \times 4\text{mm}$ (we
117 adjust the size depending on the size of the insect). This weighs about 5mg .³ Using tweezers we fold it in half and
118 spread the ends of the two halves apart, so the reflector has a small ridge. This helps the RTS detect the bee from a
119 wider range of angles. Using tweezers to hold the reflector by the ridge we apply a small amount of cyanoacrylate
120 adhesive (Loctite superglue) to the reflector and affix it to the thorax of the insect. We cut small notches in each
121 tag prior to attachment, to allow later unique reidentification of each bee by a human observer.

122 **Commercial Nests** A similar process to the above was used for tagging the bees from the artificial nests (Biobest,
123 standard hive).

124 **2.3 The System**

125 Several iterations of the RTS have been constructed. Here we describe the most advanced.

126 **Computer** The system uses a raspberry pi for controlling the flashes and camera and for processing and saving the
127 camera output (Pi 4 model B, Raspberry Pi Foundation).

128 **Interface board** A very simple PCB interface board provides the connection to the pi's GPIO pins and allows the

³This can be made lighter if required by removing the fabric on the reverse of the reflector.

129 different components to be connected (battery pack, voltage regulator, camera trigger and power, flash triggers and
130 raspberry pi).

131 **Camera and Lens** The most important aspect of the camera (the monochrome CMOS 2064 × 1544 GCC2062M,
132 smartek) was that it must have a global electronic shutter. This allows very brief exposures (e.g. 25 μs) just covering
133 the duration of the flash. A standard machine vision 2 megapixel lens was used (Kowa LM5JCM 2/3" 5mm F2.8
134 C-mount, Kowa American Corp.)

135 **Flash** Two or four flashes were used (TT560, Neewer, set to 1/16 power), either configured to fire in unison or
136 sequentially. In the former the flash power is greater, thus potentially increasing the range of the system, but in the
137 latter the system can take more photos as the flashes can sequentially recharge.

138 **Power source** The pi and camera were powered from 10 AA rechargeable batteries (eneloop pro, panasonic). We
139 used a 5V voltage regulator to provide the pi's power (3A 5V, UBEC, hobbywing). The camera itself was powered
140 directly from the battery pack. The flashes each contain 4 AA batteries.

141 2.4 Algorithm and Software

142 2.4.1 Overview

143 To find a retroreflective tag in the photographs requires some image processing. At its simplest, the algorithm needs
144 to (a) Align the flash and no-flash photos together (b) Subtract the no-flash photo from the flash photo (c) Find the
145 brightest point. This simple algorithm is fairly successful, however we found false positives were being frequently
146 detected. For a reobservation study in which a true positive is relatively rare, the false positive rate needs to be
147 very low to avoid masking the rare true positive events.

148 We found false-positives (FPs) had a variety of causes. The most common were moving bright objects or features.
149 These include the pattern of leaves and branches moving against the relatively bright sky leading to bright dots
150 appearing and disappearing regularly in the subtracted image. Similarly reflective objects such as lamp posts, plant
151 pots etc, often had reflections which led to bright pixels in the subtracted image. Humans or other animals moving
152 within the scene could also lead to differences in the flash/no-flash photos. We also found occasional near-camera
153 (out of focus) particles (possibly wind-carried seeds or pollen) were being brightly illuminated by the flash.

154 A three stage approach was taken to remove various types of FP event. First, rather than just subtract the
155 non-flash photo, this photo is maximum-dilated (see supplementary) to ensure that small movements in the location
156 of bright spots will still lead to them being cancelled in the flash photo. For example, a bright flower moving in the
157 wind, or the dots of sky visible through a tree, can move between the two photos. The camera itself may also move
158 slightly. By dilating the no-flash photo these bright dots will still be subtracted from their counterparts in the flash
159 photo.

160 Second, some objects such as litter, a swinging bird-feeder, street signs, or other reflective objects do produce

161 a bright reflection, which will appear in the flash/no-flash subtracted image. We handle this by noting that
162 foraging bees rarely remain in the same location for long. Thus by combining (finding the maximum of) previous
163 flash/no-flash subtractions, and then subtracting *this* from our current flash/no-flash image, we remove all the
164 stationary sources of reflection.

165 Third, some objects may still appear, even in this resulting image. Examples include motes of pollen or
166 wind-transported seed; moving retroreflectors such as car number plates etc, or humans and other animals moving
167 about the scene. The retroreflector is far smaller than a pixel so leads to a very concentrated bright ‘blob’ of just a
168 few pixels. Most other false positives that remain at this point are typically considerably larger. We used a machine
169 learning classifier to identify and remove these remaining false positive targets.

170 2.4.2 ML Classifier Training

171 We visited two locations over five days (and used several camera orientations) and used a retroreflector on the end
172 of a one-metre bamboo cane. We took photos of the reflector at various distances up to 40m, holding the reflector
173 at different heights. We labelled 812 images. In each we specified the location of the retroreflector (easily identified
174 as we could visually inspect the image and find the fieldworker holding the stick). We also automatically found
175 another 7000 maximums in the difference images that were not the retroreflector. We then used six features (see
176 below) associated with each of these points to train a (linear kernel) support vector machine to distinguish between
177 the two classes.

178 2.4.3 The Algorithm

179 The algorithm for detecting the bee consists of the following steps:

- 180 1. Capture: Regularly (between every 0.25 to 6 seconds) a set, S_i , of photos are taken. These sets we index:
181 $i = 1..n$. We assume we are searching for the bee in the latest set, S_n . Within each set S_i there is one photo
182 with the flash (F_i) and at least one without ($NF_i^{(1)}, NF_i^{(2)} \dots$). These are typically taken within 2ms of each
183 other. We typically take the no-flash photo(s) first (to ensure the flash is not lit). Later, during analysis, we
184 found a single no-flash photo was sufficient.
- 185 2. Alignment: A coarse or approximate alignment may be necessary within and between pairs of images if the
186 RTS’ platform is not stable (for example on the tethered balloon). This can be done using a standard library
187 (OpenCV) or for translation-only we found a convolution of a low-resolution version of the image provided
188 very fast coarse-alignment.
- 189 3. Subtraction (for current set S_n): For the current set, S_n , we maximum-dilate, $D_M(\cdot)$, (see below) each of the
190 non-flash photos, which is then subtracted from the flash photo. The minimum A_n over these subtracted pairs
191 is computed (where the min operator is per pixel), so for pixel k , $[A_n]_k = \min_j \left[[F_n - D_M(NF_n^{(j)})]_k \right]$

- 192 4. Subtraction (for all previous sets S_i , $i \in 1..n - 1$): For each previous set, S_i , we don't dilate either image,
 193 we just subtract each of the non-flash photos from the flash photo. The *maximum* B_n over all these
 194 subtracted pairs, from all the previous sets, is computed (where the max operator is per pixel), so for pixel k ,
 195 $[B_n]_k = \max_{i \in 1..n-1} \max_j \left[[F_i - D_M(NF_i^{(j)})]_k \right]$. The maximum per set can be cached as it is used repeatedly.
- 196 5. Overall subtraction: We apply the maximum-dilate operation to the maximum subtraction image B_n from the
 197 previous sets and subtract this from the current image to give us our resulting search image, $R_n = F_n - D_M(B_n)$.
- 198 6. Finding Candidate Patch Features: We iteratively find the location of the maximum pixel p in R_n : $p =$
 199 $\operatorname{argmax}_k [R_n]_k$. For this maximum point we record six features:

- 200 • The value of the maximum, $[R_n]_p$
- 201 • The value of the subtracted pair's pixel $[F^{(n)} - NF_1^{(n)}]_p$.
- 202 • The background mean: The average of the 20×20 patch surrounding the maximum pixel, p , excluding a
 203 central 7×7 square.
- 204 • The maximum of wider surrounding points: We find the maximum pixel value of 8 evenly-spaced pixels
 205 placed in an 8×8 square around p .
- 206 • The maximum of closer surrounding points: We find the maximum pixel value of 8 evenly-spaced pixels
 207 placed in an 4×4 square around p .
- 208 • Centre sum: The sum of pixel p and its four neighbours.

209 We then delete a 15×15 square centred on p , and repeat the search for candidate patches. Typically we
 210 generate 20 candidate patches.

- 211 7. We finally use these six features to query a support vector machine classifier, previously trained on manually
 212 generated and labelled data. This gives a score/confidence for each of these candidate patches. We select a
 213 threshold depending on the application.

214 2.5 3D flight path reconstruction

215 A single RTS can only resolve a tag's location to a vector, whose origin is at the camera and with a direction
 216 determined by the tag's position in the photo. If the same bee is tracked simultaneously using two tracking systems
 217 placed at different locations, the flight path of the bee can be reconstructed by combining this series of vectors.

218 Our final experiment used two RTS to compute the flight path of a bee, to demonstrate this as a possible
 219 application. After placing the two RTS, nine unique landmarks were identified in the photos from the two systems,
 220 and used to place the two cameras in 3D. Specifically, the orientation of the cameras was manually chosen and
 221 so was fixed in the model, however the relative positions of the two RTS was optimised inside the model. Ideally

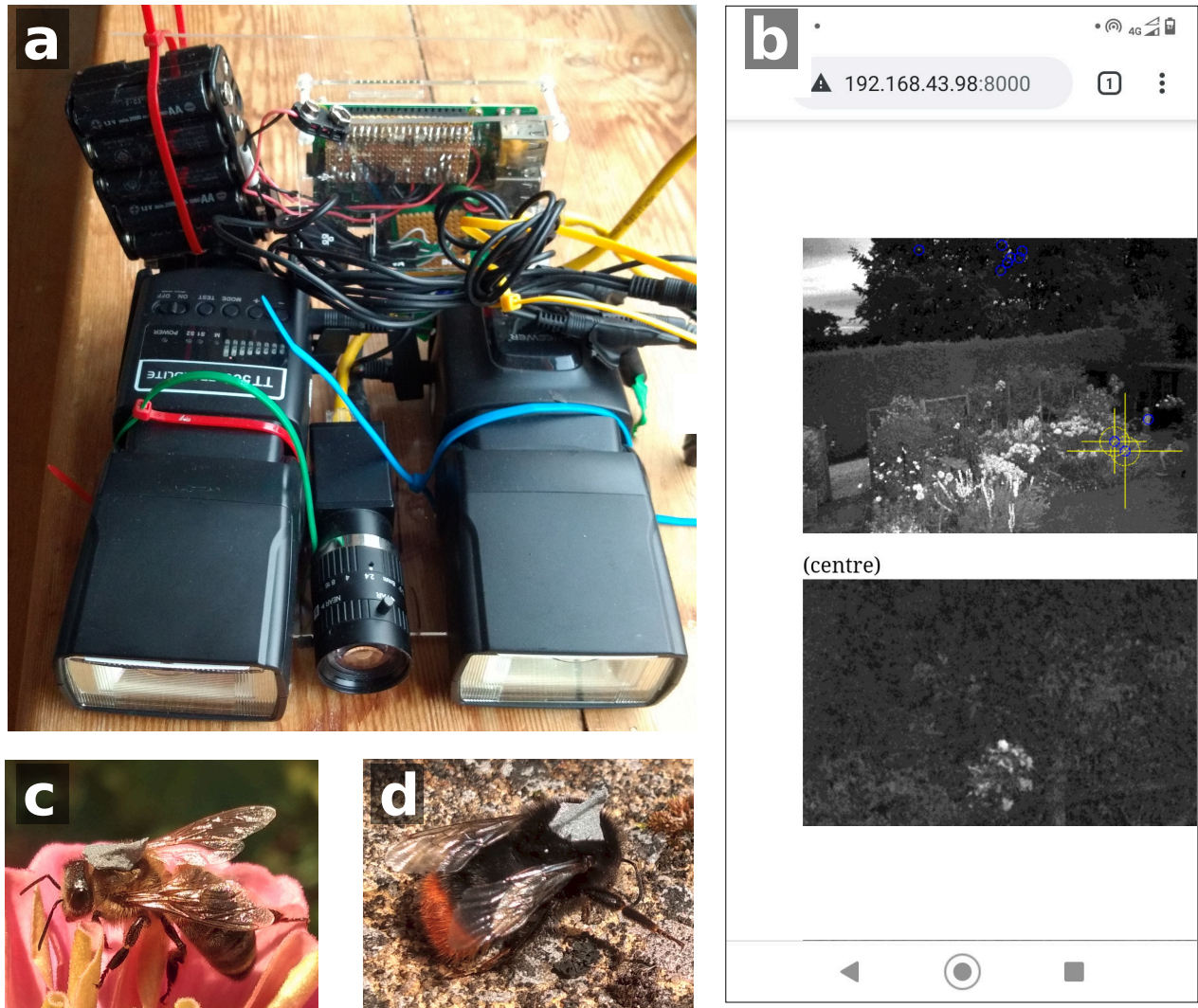


Figure 2: a. The complete tracking system. In the foreground are the two flashes and the camera. Mounted on the back is the raspberry pi and the AA battery packs. b. Screenshot of part of the webinterface illustrating realtime target tracking. The yellow crosses with circles are the locations where the system has confidently found the tags. The candidate locations it checked are marked with blue circles (mainly included to support algorithm development). The lower image is simply the central portion of the image, used to ensure the lens is focused (only really necessary after the system's initial construction). c. A tagged *Apis mellifera*, d. A tagged *Bombus lapidarius*.

222 the two vectors associated with each landmark should intersect. However aberration, slight mislabelling and other
223 factors can lead to small discrepancies. The model RTSes are placed to minimise the error. The distances between
224 landmarks are known allowing us to calibrate the model.

225 When accessed through the web interface, the RTS software automatically requests the date and time during
226 initialisation and sets its internal clock. Given the low-latency of the wifi connection to the mobile phone or laptop,
227 the two tracking systems should have a relative accuracy of within 2ms.

228 Reconstructing the flight path isn't simply a matter of triangulation as the photos are taken at different times.
229 We solve this using a simple approximation in this paper, but describe a more appropriate method for further work
230 in the Discussion.

231 In the field trial, one RTS was the new system capable of 4 acquisitions per second, while the older system
232 only ran every two seconds. So as a simple approach, the old system's vectors are interpolated for each of the new
233 system's. Then the nearest point to these two vectors, that lies equidistant between them, is assumed to be the
234 bee's location.

235 We finally use these coordinates as training points in three independent Gaussian processes (with the Exponenti-
236 ated Quadratic kernel), parameterised by time, with appropriate priors regarding plausible acceleration (specifically
237 a lengthscale of 1.5s was chosen for each axis).

238 2.6 Field Sites

239 For the evaluation phase we used Site A ($53^{\circ}22'16.6''$ N, $1^{\circ}30'49.7''$ W) and Site B ($53^{\circ}22'16.7''$ N, $1^{\circ}30'45.1''$ W).
240 These are both on a quiet suburban private road with a backdrop of buildings, trees, parked cars and plants. We
241 used these with the aim of providing a relatively challenging environment for the RTS during the evaluation. The
242 case studies were conducted at: Site C, an experimental ornamental urban meadow ($53^{\circ}22'46.2''$ N, $1^{\circ}26'09.7''$ W);
243 Site D, a small wild-flower area in a landscaped university campus ($53^{\circ}22'17.9''$ N, $1^{\circ}30'26.1''$ W); Site E, a garden
244 on the edge of the small, rural town of Minchinhampton, Gloucestershire ($51^{\circ}42'34.8''$ N, $2^{\circ}10'31.0''$ W); Site F, a
245 garden in the village of Chedworth, Gloucestershire ($51^{\circ}47'51.2''$ N, $1^{\circ}55'03.7''$ W).

246 The 3D reconstruction experiment, at Site G, was on a lawn at another part of the university campus, surrounded
247 by trees and a nearby small allotment ($53^{\circ}22'21.5''$ N $1^{\circ}30'08.4''$ W).

248 3 Results

249 3.1 Evaluation

250 The supplementary includes a calculation of the theoretical range but we were interested in what the system could
251 achieve in real conditions. To perform the evaluation we trained the classifier on a smaller subset of the images
252 from one day and location (Site A). This classifier was used in the pipeline to detect the retroreflector in images

| (training data) | | Actual | |
|-----------------|----------|----------|----------|
| | | Positive | Negative |
| Predicted | Positive | 90 | 0 |
| | Negative | 14 | 2456 |

| (test data) | | Actual | |
|-------------|----------|----------|----------|
| | | Positive | Negative |
| Predicted | Positive | 57 | 1 |
| | Negative | 6 | 1736 |

Table 1: Evaluation of the RTS on labelled data. Upper tables when applied to the data used for training. Lower table when applied to new test data (from a different location and day).

| Distance | Flashes | threshold<0 | | threshold<-1 | | threshold<-2 | |
|----------|---------|--------------|------------|--------------|-----------|--------------|-----------|
| | | TP rate | FP rate | TP rate | FP rate | TP rate | FP rate |
| 15m | 2 | 89% (17/19) | 5% (1/19) | 74% (14/19) | 0% (0/19) | 47% (9/19) | 0% (0/19) |
| 24m | 2 | 100% (16/16) | 0% (0/16) | 88% (14/16) | 0% (0/16) | 88% (14/16) | 0% (0/16) |
| 30m | 2 | 67% (12/18) | 17% (3/18) | 56% (10/18) | 5% (1/18) | 33% (6/18) | 0% (0/18) |
| 30m | 4 | 100% (25/25) | 12% (3/25) | 72% (18/25) | 8% (2/25) | 68% (17/25) | 0% (0/25) |
| 39m | 2 | 57% (4/7) | 57% (4/7) | 14% (1/7) | 0% (0/7) | 0% (0/7) | 0% (0/7) |
| 39m | 4 | 44% (8/18) | 17% (3/18) | 22% (4/18) | 6% (1/18) | 6% (1/18) | 0% (0/18) |

Table 2: Effect of distance and number of flashes on detection rate (TP rate = True Positive rate, FP = False Positive rate). The rate is per image, an image can have both a true positive and a false positive (e.g. if two locations were identified by the tracking system as being a tag). The more negative thresholds are less likely to assign a bright spot a ‘positive’ target.

253 from a second day at Site B. The reflector in both was moved between photos at varying locations and distances
 254 between approximately 25m to 40m away.

255 Table 1 displays a confusion matrix of the system on the training and test data. Over 90% of the test data
 256 points were correctly detected. There was one false positive, upon inspection this was caused by the bright reflection
 257 from the watch of a passer-by.

258 We next reversed the training and test datasets (training using Site B and testing on the data from Site A).
 259 The test data samples from Site A had their distances and the use of either two or four flashes recorded. Table 2
 260 illustrates the true and false positive rate, for three choices of classifier threshold. This provides a trade-off between
 261 detecting hard to spot distant bees, and avoiding false alarms. One might wish to avoid false alarms by using a
 262 threshold of -2, which in this test data found zero false positives. We found that the RTS worked to approximately
 263 35m. Obviously the presence or absence of objects that generate false positives, the size of the reflector, the amount
 264 of daylight and other factors are also relevant. The sudden loss of signal between 30 and 39 metres relates to the
 265 $1/d^4$ relationship with reflected signal strength, the 30% increase in distance equates, in theory, to a 65% reduction
 266 in signal strength. We note that in this table and in later field work, where the bee was within 20m, the classifier
 267 did not detect the bee, as it appeared ‘too bright’. Some of the plots in Figure 3 demonstrate this. Relatively little
 268 training data included samples with this proximity. Provisioning additional, more varied training data will likely
 269 solve this. In our case we used an additional non-ML heuristic for these very bright spots.

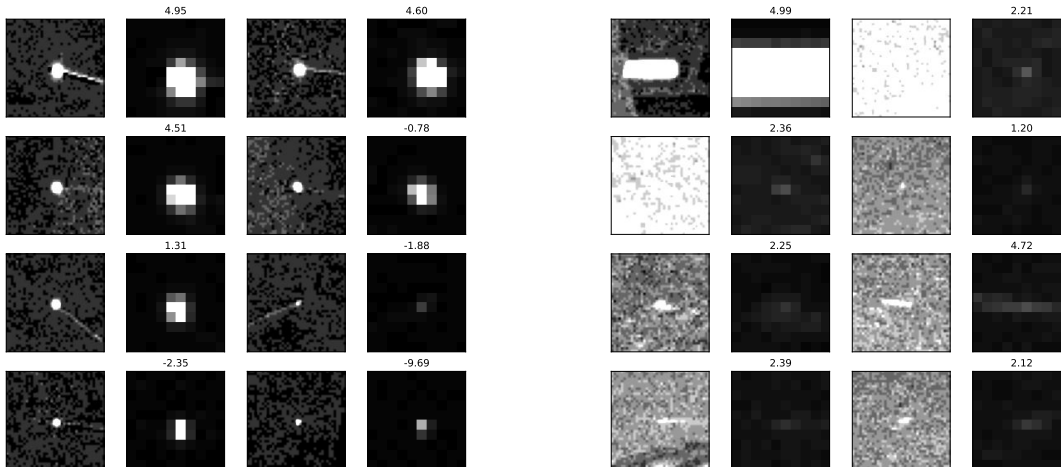


Figure 3: Samples of true (left) and false (right) targets. The first and third column of each are 40×40 greyscale images (white=5, black=0) centred on a maximum point. The second and fourth columns are 10×10 enlarged images (white=50). The value in the title is the classifier score (negative = more confident).

270 3.2 Case Studies

271 Before looking at tracking, floral preference and 3D trajectories, it is worth looking at the detection of single, tagged
 272 bees, as these case studies provide simple, clear examples of the utility of the RTS.

273 3.2.1 Aerial (tethered balloon) Platform

274 An early version of the RTS was deployed in 2018 using a tethered balloon (see Figure 4b) to test the use of an
 275 aerial platform. This experiment was conducted at Site C. We first tagged a *Bombus terrestris* male, found on
 276 a *Heuchera villosa*. We released the bee on the same plant. After a period of feeding it left. Within an hour it
 277 was detected returning to the plants. Figure 4a illustrates the detection and tracking. It was first detected above
 278 the field (at 13:12:32). It was then detected in the planting area (at 13:13:51 and every four seconds after⁴). To
 279 confirm the tracked object was real and our tagged bee, we visited the location identified by the system and found
 280 the tagged bee (figure 4c) feeding on a *Sedum telephium* not far from the plant upon which it was released. This
 281 provided the first demonstration that the system could detect and track a bee.

282 The balloon platform was found to be unstable in even slight wind, so in 2019 and 2020, ground based platforms
 283 were used with an additional ‘ridge’ added to the tags to ensure they remained visible from a lower elevation. The
 284 view from the balloon platform did make it easier to localise the bee.

⁴The delay prior to this second detection was due to users infrequently attending the real-time imagery. The system at this stage did not produce a sound when a detection occurred.

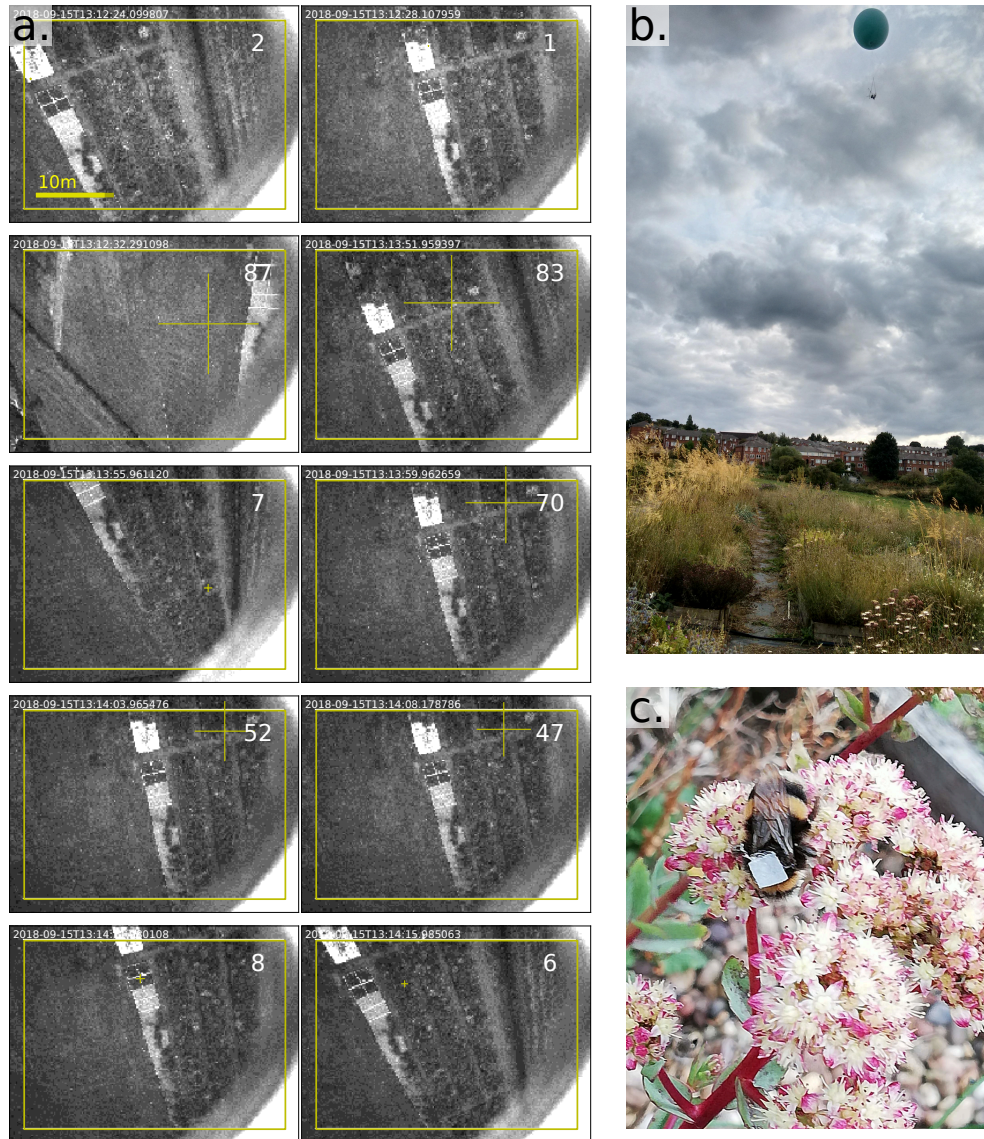


Figure 4: a. Tracking tagged *Bombus terrestris*. Score displayed in top right of each image (over 25 indicates a confident detection). Cross-hair size scaled by score. A returning tagged bee detected as it flew across field (second row, left column) and settled in the planting (second row onwards). Due to wind the camera was at a problematic angle in some of the images. b. The tracking system suspended from the tethered helium balloon. c. The tagged bee, rediscovered using the tracking system. NB: The earlier reflectors were simple flat squares.

285 **3.2.2 First field trial: Bumblebee re-observed in pine tree**

286 Our first field trial with the current RTS was with a wild worker *Bombus terrestris* which we caught foraging in a
287 mini-meadow area at Site D (Figure 5e). It was tagged (Figure 5a & 5b) and released. We monitored the wild-flower
288 area at the site with the tracking system, anticipating the bee would return to the forage. However the system
289 unexpectedly found it 3m above the ground in a pine tree, 33m from the tracking system (Figure 5c & 5d).

290 Figure 5d illustrates reflections from other objects (a lifebuoy cover and the retroreflective material on a traffic
291 cone). Although both of these objects reflected the flash, they were stationary, and so were cancelled by subtracting
292 previous image pair differences (step 5 in Section 2.4.3). They would also have been removed by the classifier due to
293 their extent and shape.

| Plant | Detection events | Percentage | Normalised Percentage |
|---------------------|------------------|------------|-----------------------|
| Clematis | 4 | 1% | 2% |
| Rosa | 2 | 1% | 0% |
| Salvia | 2 | 1% | 1% |
| Solidago | 10 | 3% | 9% |
| Crocosmia | 0 | 0% | 0% |
| Pelargonium | 1 | 0% | 1% |
| Rudbeckia | 0 | 0% | 0% |
| Alstroemeria | 2 | 1% | 1% |
| Acanthus | 15 | 5% | 10% |
| Phlox | 52 | 16% | 22% |
| Verbena bonariensis | 13 | 4% | 9% |
| Campanula | 2 | 1% | 1% |
| Dahlia | 64 | 19% | 15% |
| Nepeta | 139 | 42% | 26% |
| Verbascum | 25 | 8% | 3% |
| Fuchsia | 0 | 0% | 0% |

Table 3: Number of times a tag was detected in proximity to each flower species over the 3 hours 23 minutes. Normalising performed by dividing count by patch area in photo.

3.2.3 *Megachile* sp. and *Apis mellifera* Tagged and Re-observed

In Sections 3.3 and 3.4 most of bees tagged were *Bombus* spp., however (at Site E) we did also find and tag a *Megachile* sp., foraging on a yellow *Dahlia* sp. See Figure 6b. The floral preference experiment below involved using the tracking system to quickly find the tagged bees and then manually uniquely identify the individuals. On two occasions the tagged *Megachile* sp. was re-identified using the system, once on the same area of *Dahlia* as it was originally foraging on (Figure 6d), and once on a nearby *Verbena bonariensis*. This case study demonstrated that the retroreflectors can be used on smaller bees than *Bombus* spp. At Site F we tried tagging four *Apis mellifera* but with less success due to the species' relatively small thorax. However using the RTS we found one of them, 210 minutes later, foraging on the same patch of *Echinops ritro* that we caught it on originally (Figures 6a and 6c). The smaller retroreflectors reduce detection range, but not as severely as one might expect. This we speculate is due to the $1/d^4$ relationship in signal strength. For example the tag on the *Apis mellifera* probably has only $4mm^2$ visible, compared to a typical tag on a *Bombus* sp. that might have up to $20mm^2$ visible. The reduced size is equivalent in terms of simple signal strength to a 33% reduction in distance (e.g. if the RTS works to 30m with the large tag, it will work to about 20m with the smaller tag). The *Apis* was detected approximately 16m from the RTS.

3.3 Tracking Foraging Bees

At Site E, we tagged 18 wild bees, picked largely at random, but with a slight selection preference towards tagging a variety of species. The tagging took place on August 2nd and August 3rd. We ran the RTS on the 2nd, 3rd and 5th. Most of this time it was being used to locate bees for the floral preference study (see Section 3.4 but data was recorded over a cumulative time of 3 hours, 23 minutes. In that time the system stored 1303 flash photo pairs and

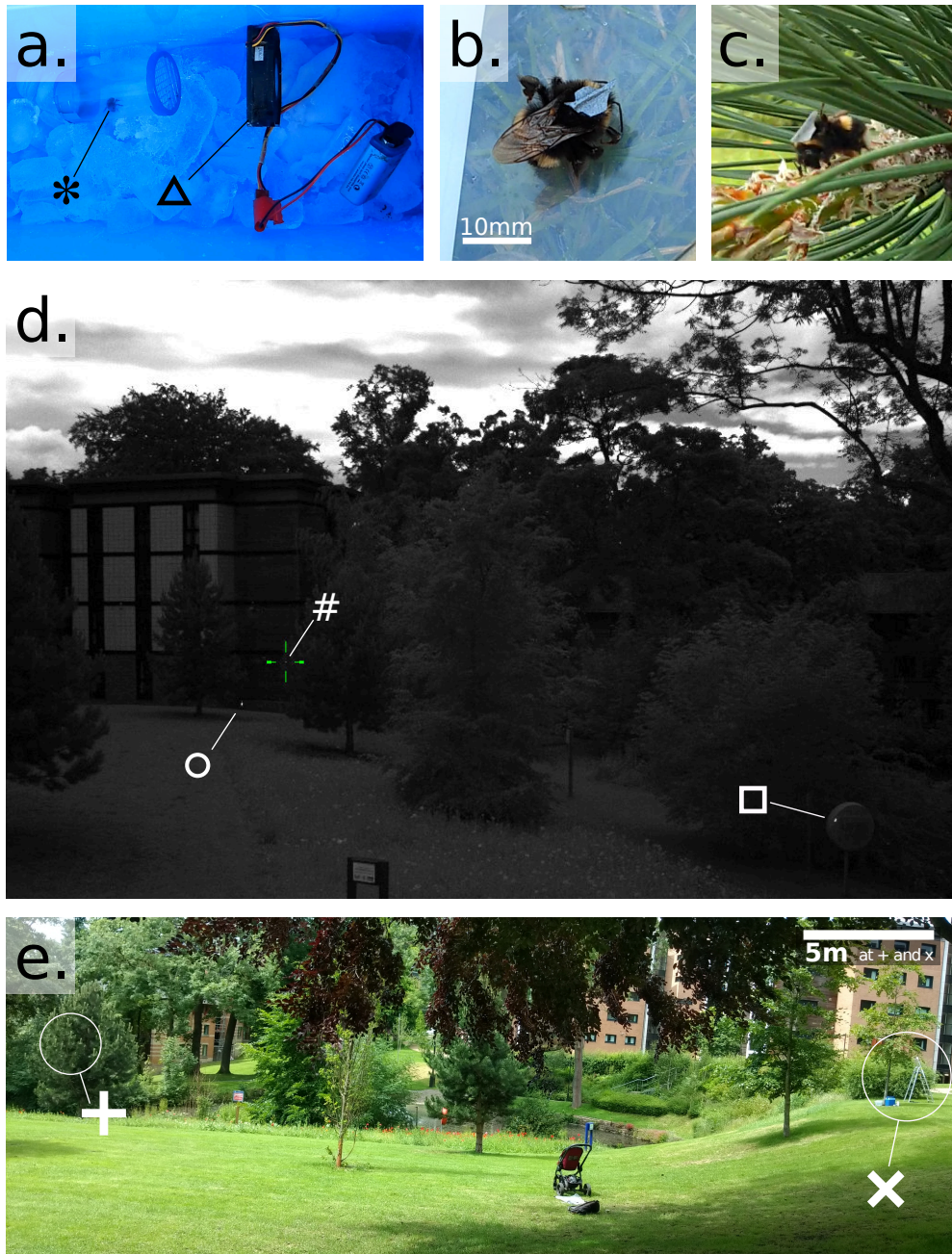


Figure 5: a. Tagging bees in the field using an icebox of salt/ice, a marking pot with mesh at both ends (*) and an electric fan (Δ). b. Tagged *Bombus terrestris*. c. The same bee having been detected in the pine tree. d. Image from tracking system, with the bee detected (#) and examples of other reflections: a lifebuoy cover (\square) and the retroreflective material on a traffic cone (\circ). e. The pine tree where the tagged bee was detected (+) and the tracking system (\times).

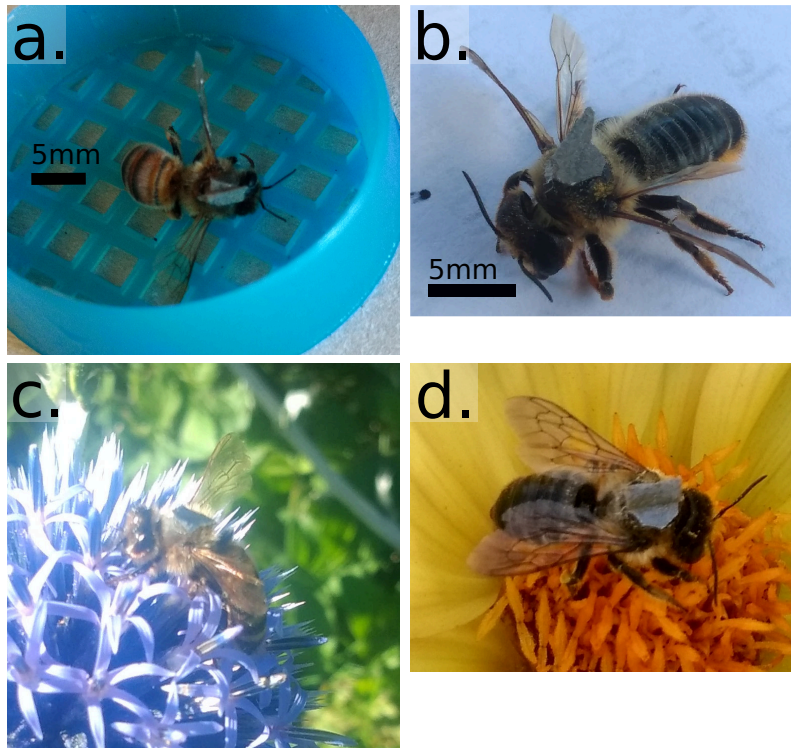


Figure 6: Newly tagged *Apis mellifera* (a) and *Megachile* sp. (b). c. The *Apis mellifera* later found foraging on a *Echinops ritro*. d. The *Megachile* sp. later found foraging on a *Dahlia* sp. flower.

313 acquired approximately 418 confirmed detections. These were semi-autonomously merged into 36 tracks (median
 314 length, 7 detections, min=1, max=45). These are plotted in figure 7. Some of the tagged bees will be responsible
 315 for several of these tracks.

316 Besides providing an example of how one can use the system for monitoring high-resolution foraging behaviour
 317 we also used the raw data to investigate the time spent on various foraging resources. Importantly this approach
 318 allows an automatic allocation of foraging time: We segmented the image into plant species using a simple interface
 319 that allowed us to click on the image to enter a ‘cloud’ of points for each species which were then used with the
 320 nearest neighbour algorithm to assign the forage each bee was using. Figure 8 illustrates the plants available for
 321 forage and their locations. As the camera orientation changed a little over the three days, we also recorded the
 322 locations of landmarks in the different sets of images (from different days) to allow automatic registration.

323 Table 3 shows the time spent on each plant type. One might wish to normalise by land area (e.g. Tasker et al.,
 324 2020), number of flowers or flower units (e.g. Urbanowicz et al., 2020). In this case we normalised by the visible area
 325 for each plant species. Ideally one would also restrict the count to those patches that have large numbers of open
 326 flowers. These issues aside, as a demonstration of the method, the table shows that there is a considerable preference
 327 for time spent foraging on *Nepeta*, *Dahlia* and *Phlox*. Obviously this is a function of both floral preferences of
 328 the tagged bees and of which flowers were available at the start of August. Note also that a small percentage of
 329 detection events will be due to a bee travelling past a floral patch, rather than foraging on it. One could further



Figure 7: The paths of bees detected using the RTS. Each line represents one track (some colours may appear similar but this does not imply the bee was the same). Foraging area extended from 8m to 15m from the tracking system.



Figure 8: The plants available for forage

| | Bee Id. | | | | |
|-----------------------|---------|-----|----|----|---|
| | #23 | #30 | #6 | #7 | |
| Fuchsia ‘Garden News’ | 1 | 0 | 0 | 0 | 1 |
| Nepeta sp. | 0 | 0 | 2 | 1 | 3 |
| Stachys byzantina | 0 | 4 | 0 | 0 | 4 |
| | 1 | 4 | 2 | 1 | 8 |

| | Bee Id. | | | | | | | | | |
|-------------------------|---------|----|----|-----|-----|-----|-----|-----|-----|----|
| | #32 | #1 | #4 | #36 | #18 | #21 | #22 | #27 | #28 | |
| Nepeta | 5 | 0 | 0 | 0 | 1 | 0 | 0 | 1 | 0 | 7 |
| Salvia ‘Hot Lips’ | 0 | 0 | 0 | 0 | 0 | 0 | 0 | 0 | 4 | 4 |
| Verbena bonariensis | 0 | 0 | 0 | 0 | 0 | 1 | 0 | 0 | 0 | 1 |
| Agapanthus africanus | 1 | 1 | 0 | 0 | 0 | 0 | 0 | 0 | 0 | 2 |
| Dahlia ‘Bishop of York’ | 2 | 0 | 0 | 1 | 1 | 3 | 2 | 0 | 0 | 9 |
| Stachys byzantina | 0 | 0 | 1 | 0 | 1 | 0 | 0 | 0 | 0 | 2 |
| | 8 | 1 | 1 | 1 | 3 | 4 | 2 | 1 | 4 | 25 |

Table 4: Contingency tables for individual bee flower visits for *B. hortorum* (upper table) and *B. terrestris* (lower table). Other species had fewer than four visits each.

process the data to remove these (e.g. by requiring two consecutive detections in the same plant area), but the strong preferences in foraging activity are visible in even the raw data. To compare with anecdotal forage preference estimates, we asked the owner of the garden to recall the top three plant species over August they felt were most popular with bumblebees. They suggested: Nepeta, Dahlia and Verbascum. This fits quite closely with our results but with Phlox instead of Verbascum. This suggests that the automatic monitoring results reflect plausible foraging activities.

3.4 Floral Preference

To provide a demonstration of the RTS being used to assist with a mark-reobservation study, we ran a simple experiment over the three days to investigate floral preference. Individual floral preference is a well known feature of *Bombus* sp. (e.g. Wilson and Stine, 1996). We wished to test whether or not individual bees have a preference for particular flowers in our study (compared to their species’ average). We left the system running over a cumulative 11 hours over the three days. While it was running the field worker was largely occupied by other activities, however the system would alert him via a sound from the mobile phone web interface to the detection of a bee. The web interface would show a cross marking the recent location of the bee, allowing him to quickly find the bee and take photos (using a standard camera) for later unique identification (using the shape of the tag).

Overall 22 tagged bees were re-observed using this approach, 54 times. For each reobservation the unique bee and its forage were recorded. Not all bees were recorded that were detected - some left before the field worker reached their location, or sometimes multiple bees were detected simultaneously.

We grouped those uniquely identified by species of bee, and constructed contingency tables (bee ID vs flower species, see Table 4). We excluded observations in which a previous observation for the same bee was within 10

350 minutes, to avoid correlations due to temporal proximity. We wish to test whether bees have individual preferences
351 for particular flower species. If individuals have no floral preference we would expect no interaction in the contingency
352 table: the expected proportion of visits to a given flower should be the same for all unique bees (this is our null
353 hypothesis). We note that in practice, preferences might be driven by subspecies differences, caste, or temporary
354 environmental differences. As a simple test to demonstrate the RTS it should suffice.

355 Clearly the expected and observed numbers in the cells of these contingency tables are small, so the χ^2 test is
356 inappropriate. We instead used the Exact Fisher Test.⁵ We only had enough samples to perform this analysis for
357 two species, We found for both *Bombus hortorum* ($p < 0.01$) and *Bombus terrestris* ($p < 0.001$) that there was
358 significant individual preferences for particular forage species beyond that expected by chance (i.e. if the species
359 had the same preference for each plant type).

360 **3.5 3D flight trajectory**

361 A final brief experiment used two RTS to compute the flight path of a bee (Figure 9b), to demonstrate this as a
362 possible application. We used a *Bombus terrestris* subsp. *audax* commercial nest (Biobest, standard hive, no cotton
363 wool) and tagged workers using the retroreflective tags. We placed the nest at Site G and positioned two RTS units
364 facing the nest, approximately 15 metres from the nest and from each other. The nest had been open for a couple of
365 days, so the workers had been foraging and had gained familiarity with the landscape. We started photographing
366 with two RTSES as we saw workers depart (Figure 9d). The bee whose successful track we captured flew briefly
367 North but turned South East (Figure 9a) and quickly accelerated (to a recorded speed of about $6ms^{-1}$), gradually
368 climbing to an approximate height of 2.5m (Figure 9c) before leaving the field of view of one of the cameras. We
369 failed to record other flights mainly due to problems with the nest. This should be considered a proof-of-concept
370 experiment.

371 **4 Discussion**

372 Over the last 25 years several methods have been developed to directly track individual insects. These methods all
373 use an electronic tag, either producing an active radio signal or passively providing a radar reflection. The RTS
374 described in this paper is quite different, relying on a small, very-low-cost, simple retroreflective tag. The main
375 disadvantage of the approach is the method's limited range (currently about 35m) which is less than for some of the
376 electronic-tag methods. But its advantages complement those methods: First, the tag itself is very small, simple and
377 low-cost, and doesn't require the awkward aerial of the electronic devices, and we found no evidence of behaviour
378 change while foraging in a small experiment (although care must be taken if using cotton-wool as insulation in an
379 artificial hive). The majority of bee species in the UK would probably find the electronic tags too cumbersome.

⁵ $M \times N$ contingency implementation thanks to Noutahi (2018), using MCMC sampling to compute the p-value.

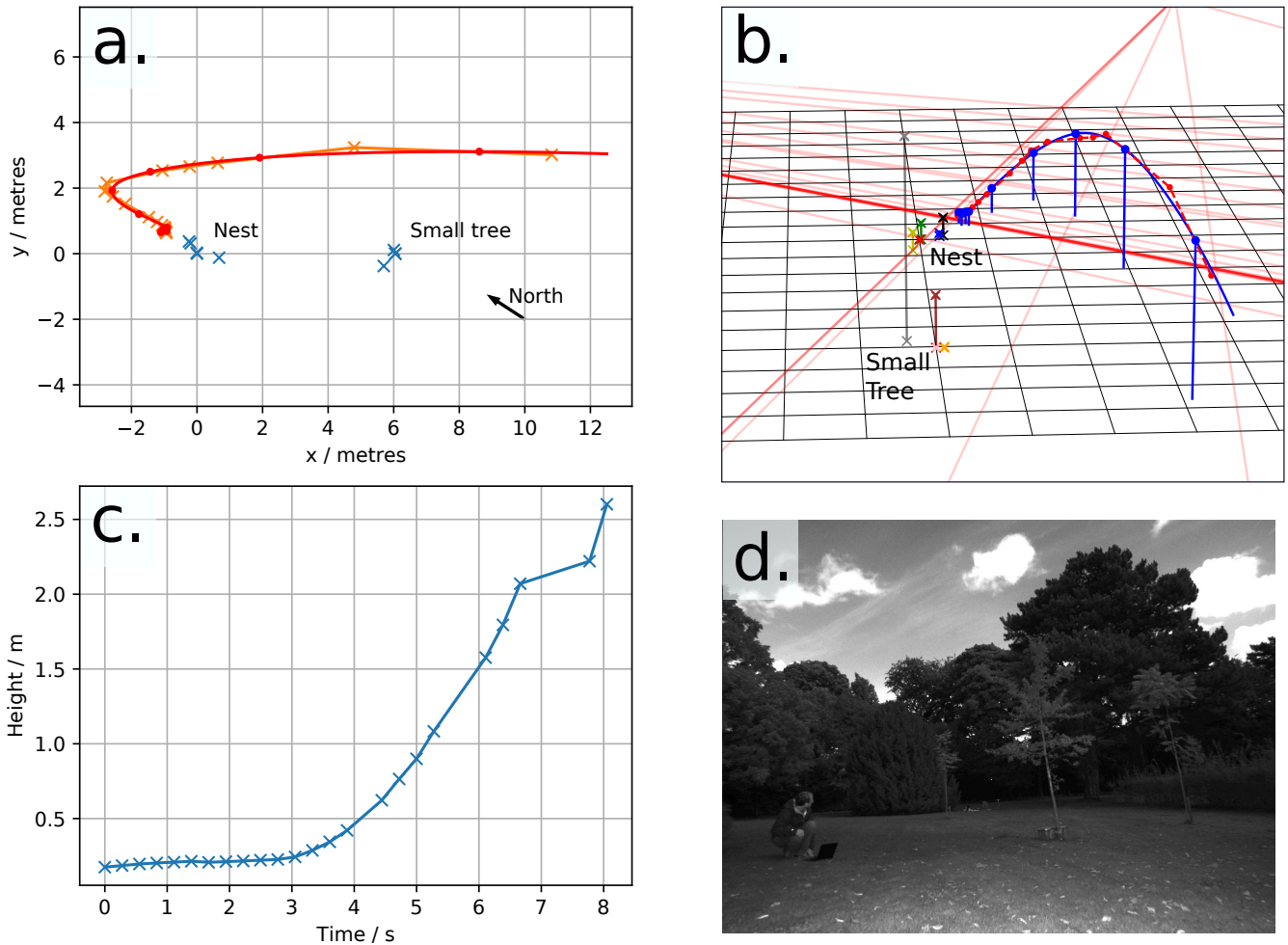


Figure 9: Reconstructed 3D flight trajectory. a. top-down projection of flight path. Orange line and crosses, the estimated observation locations. Red line and circles, fitted path with markers each second. Blue crosses, landmarks. b. 3D perspective projection. Dashed red line and circles, estimated observation locations. Blue line and circles, fitted path with markers each second. Crosses and vertical lines, various landmarks. Red lines indicate vectors centred on the two cameras, each associated with an observation. Ground plane grid squares 1×1 metres. c. Height of bee during flight. d. Photo taken from new pi 4 tracking system. The researcher and nest are in the foreground a tagged bee is illuminated and visible near the centre of the frame. The ‘small tree’ landmark is the tree to the right of the image.

380 Given that we were able tag and track an *Apis mellifera*, it is likely that the retroreflective tag could be used with
381 many other species of bee of around this size.

382 We found the simple, initial experiment: tagging a foraging *Bombus terrestris* and using the RTS to later detect
383 the bee in the pine tree, was particularly convincing as to the method’s effectiveness. The tree would not have
384 been a location we would have looked for the bee, if trying to re-observe during a transect. Even if the bee had
385 returned to the wild-flower area, finding it manually would have been laborious and unreliable. The simplicity and
386 effectiveness of the detection demonstrates the benefits the system can bring to re-observation studies in particular.

387 To move beyond single case-studies, we performed a simple floral preference experiment and demonstrated
388 the automatic monitoring and tracking that the system can provide. We also demonstrated in a proof-of-concept
389 experiment how one can combine data from two systems to infer the bee’s flight path in 3D.

390 There are a considerable range of experiments and research questions that could be supported with this technology,
391 we just mention a few and then discuss future improvements to the underlying method.

392 4.1 Future Experiments

393 First, the most obvious initial use is as part of a standard mark-reobservation study, to increase the detection
394 rate many times of the marked bees. Indeed the system could also be left to run autonomously for long periods,
395 further increasing the rate of reobservation. Goulson (2003) wrote that ‘In more typical, patchy landscapes the
396 mark-reobservation method seems to be of little use without a huge team of observers to search for bees.’ We
397 propose that a small number of these tracking systems deployed at different locations can play the role of this ‘huge
398 team’.

399 Second, many bees only forage within 100-300m of the nest (Gathmann and Tschardt, 2002). Given the low
400 cost of the tracking system, we envisage that one could monitor the entire foraging range of such doorstep foraging
401 species by distributing several tracking systems over much of the plausible area likely to be visited.

402 Third, we found the 3D path reconstruction was relatively simple to achieve with this system, and is likely to
403 be a method of considerable interest to neuroethology, as it allows one to record in considerable detail the initial
404 learning flight of the bees, and investigate how modifications to the environment lead to changes in behaviour,
405 allowing inference to be made around the cognitive processes involved in the bee’s navigation and perception. Ideally
406 more than two tracking systems should be used together, to further refine the path, and providing some redundancy
407 to the data (see ‘Tracking in three dimensions’ on p420 in Dell et al., 2014; Straw et al., 2011).

408 Fourth, the RTS can remain in a fixed location, monitoring part of the landscape for considerable periods (with
409 occasional battery and SD card replacements being its only limit). We suggest long-term floral preference studies
410 could easily be conducted. We also noticed anecdotally that in our data we would often see several bees foraging
411 at the same time, then have a period with none. We wonder if this is chance, or due to cyclic patterns in nectar
412 depletion or possibly due to slight changes in the environment (temperature or wind). The high spatial resolution

413 could also allow many individual flowers to be monitored for tagged bees, simultaneously.

414 Finally, the system’s low cost, small size, ease of deployment and simplicity of use will give more researchers
415 greater access to direct-tracking. For example, early nest finding could be achieved by tagging a foraging queen
416 and tracking her back to the nest. One might best achieve this with the harmonic radar or VHF radio tags, but
417 access and use of these tools is quite limited. Anecdotally we have noticed how queen bees, like workers, return on a
418 similar path (or ‘bee line’) regularly to a forage patch. One could move or distribute the tracking system(s) along
419 this path to eventually discover the nest.

420 **4.2 Future Improvements**

421 We first note that some simple hardware improvements, such as mounting on a rotating platform (which we
422 experimented with previously) and using a slightly telephoto lens and a Fresnel flash lens could considerably increase
423 the area scanned, potentially to about 1 hectare.

424 The next methodological improvement we are investigating is the potential for unique bee identification by
425 combining the retroreflectors with colour filters to allow a colour camera to uniquely identify different tagged bees.
426 Further refinement could be achieved by adding additional filters to the camera flashes. This will allow, for example,
427 the floral preference study to have been run without field-worker intervention.

428 Although tagging bees with the retroreflective labels is relatively simple, it might be possible to tag all the bees
429 using retroreflective powder, using the technology described in Osborne et al. (2008) for mass-marking.

430 The capacity to take 4 photos each second developed towards the end of the research suggests that we should use
431 the sequence of images to improve the detection and tracking accuracy (both in 2D and 3D). Future work should
432 investigate the use of Bayesian approaches for such integration. A particle filter feels like an appropriate method as
433 the dimensionality of the domain is low and the state space is non-linear with a multimodal posterior. In 3D the
434 particle filter would be particularly effective as the likelihood function will consist of distributions along various
435 vectors (each associated with a bright pixel in a photo).

436 Finally, building on our earlier work using alternative platforms, we found that, as the tracking system is fairly
437 lightweight it can be used with drones, balloons and 10m masts. Each of these has its own advantages, in particular
438 one might envisage that combining with a drone could in principle allow a tagged bee to be followed across the
439 landscape. This could be combined with work such as Le et al. (2017), tracking the tagged bee with a UAV, allowing
440 the evaluation of landscape features as corridors or barriers to bumblebees, for instance.

441 **4.3 Conclusion**

442 We have presented a novel method for tracking bees using small, light-weight retroreflective tags, using low-cost
443 equipment. This method complements electronic and indirect tracking tools, for example it allows tracking of smaller

444 bees than harmonic radar or VHF radio. We anticipate the Retroreflector-based Tracking System will support a
445 wide range of ecological research.

446 Acknowledgements

447 This project was part funded by the Sheffield University Socially Enterprising Researcher grant (2016, 2017) and
448 the Eva Crane Trust (2019).

449

450 **Authors' contributions:** MTS conceived the idea for the tracking system and designed and built the system. ML
451 assisted with data collection. RC provided useful insight into bee behaviour, tagging and species identification. All
452 authors contributed critically to the drafts and gave final approval for publication.

453

454 **Data archive:** Experimental data collected during the experiment will be archived in the University of Sheffield's
455 Research Data Catalogue and Repository⁶.

456 References

457 Beil, M., Horn, H., and Schwabe, A. Analysis of pollen loads in a wild bee community (hymenoptera: Apidae)—a
458 method for elucidating habitat use and foraging distances. *Apidologie*, 39(4):456–467, 2008.

459 Bender, S. F., Rodacy, P. J., Schmitt, R. L., Hargis Jr, P. J., Johnson, M. S., Klarkowski, J. R., Magee, G. I.,
460 and Bender, G. L. Tracking honey bees using lidar (light detection and ranging) technology. *Sandia Report*
461 *SAND2003-0184*, 87185, 2003.

462 Bridge, E. S., Wilhelm, J., Pandit, M. M., Moreno, A., Curry, C. M., Pearson, T. D., Proppe, D. S., Holwerda, C.,
463 Eadie, J. M., Stair, T. F., et al. An arduino-based rfid platform for animal research. *Frontiers in Ecology and*
464 *Evolution*, 7:257, 2019.

465 Cant, E., Smith, A., Reynolds, D., and Osborne, J. Tracking butterfly flight paths across the landscape with
466 harmonic radar. *Proceedings of the Royal Society of London B: Biological Sciences*, 272(1565):785–790, 2005.

467 Capaldi, E. A. and Dyer, F. C. The role of orientation flights on homing performance in honeybees. *Journal of*
468 *Experimental Biology*, 202(12):1655–1666, 1999.

469 Capaldi, E. A., Smith, A. D., Osborne, J. L., Fahrbach, S. E., Farris, S. M., Reynolds, D. R., Edwards, A. S.,
470 Martin, A., Robinson, G. E., Poppy, G. M., et al. Ontogeny of orientation flight in the honeybee revealed by
471 harmonic radar. *Nature*, 403(6769):537–540, 2000.

⁶<https://www.sheffield.ac.uk/library/rdm/orca>

- 472 Chapman, J., Reynolds, D., and Smith, A. Migratory and foraging movements in beneficial insects: a review of
473 radar monitoring and tracking methods. *International Journal of Pest Management*, 50(3):225–232, 2004.
- 474 Charvat, G. L., Rothwell, E., and Kempel, L. Harmonic radar tag measurement and characterization. In *IEEE*
475 *Antennas and Propagation Society International Symposium. Digest. Held in conjunction with: USNC/CNC/URSI*
476 *North American Radio Sci. Meeting (Cat. No. 03CH37450)*, volume 2, pages 696–699. IEEE, 2003.
- 477 Comont, R. and Miles, S. Beewalk annual report 2019. *Bumblebee Conservation Trust, Stirling, Scotland UK*, 2019.
- 478 Connolly, C. C.N.;Moffat. The number and individual weight of bumblebees (*bombus terrestris* au-
479 dax) from nests containing neonicotinoids in wester ross, uk, 2015. URL [https://doi.org/10.5285/](https://doi.org/10.5285/341414f8-e88a-43e5-ade3-c30623c1586d)
480 [341414f8-e88a-43e5-ade3-c30623c1586d](https://doi.org/10.5285/341414f8-e88a-43e5-ade3-c30623c1586d).
- 481 Daniel Kissling, W., Pattemore, D. E., and Hagen, M. Challenges and prospects in the telemetry of insects. *Biological*
482 *Reviews*, 89(3):511–530, 2014.
- 483 Darvill, B., Knight, M. E., and Goulson, D. Use of genetic markers to quantify bumblebee foraging range and nest
484 density. *Oikos*, 107(3):471–478, 2004.
- 485 Dell, A. I., Bender, J. A., Branson, K., Couzin, I. D., de Polavieja, G. G., Noldus, L. P., Pérez-Escudero, A., Perona,
486 P., Straw, A. D., Wikelski, M., et al. Automated image-based tracking and its application in ecology. *Trends in*
487 *ecology & evolution*, 29(7):417–428, 2014.
- 488 Dramstad, W. E. Do bumblebees (hymenoptera: Apidae) really forage close to their nests? *Journal of Insect*
489 *Behavior*, 9(2):163–182, 1996.
- 490 Fischer, J., Mueller, T., Spatz, A.-K., Greggers, U., Gruenewald, B., and Menzel, R. Neonicotinoids interfere with
491 specific components of navigation in honeybees. *PloS one*, 9(3):e91364, 2014.
- 492 Fisher, K., Dixon, P., Han, G., Adelman, J., and Bradbury, S. Locating large insects using automated vhf radio
493 telemetry with a multi-antennae array. *Methods in Ecology and Evolution*, 2020.
- 494 Gathmann, A. and Tschardt, T. Foraging ranges of solitary bees. *Journal of animal ecology*, 71(5):757–764, 2002.
- 495 Goulson, D. *Bumblebees: Their Behaviour and Ecology*. Oxford University Press, USA, 2003.
- 496 Goulson, D., Peat, J., Stout, J. C., Tucker, J., Darvill, B., Derwent, L. C., and Hughes, W. O. Can alloethism in
497 workers of the bumblebee, *Bombus terrestris*, be explained in terms of foraging efficiency? *Animal Behaviour*, 64
498 (1):123–130, 2002.
- 499 Hagen, M., Wikelski, M., and Kissling, W. D. Space use of bumblebees (*Bombus* spp.) revealed by radio-tracking.
500 *PloS one*, 6(5):e19997, 2011.

501 Hawkins, H., Carlson, P., Schertz, G., and Opiela, K. Workshops on nighttime visibility of traffic signs: Summary of
502 workshop findings. Technical report, Report FHWA-SA-03-002, Office of Safety, Federal Highway Administration,
503 Washington, DC, 2003.

504 Kaftanoglu, O., Linksvayer, T. A., and Page Jr, R. E. Rearing honey bees, *Apis mellifera*, in vitro i: Effects of
505 sugar concentrations on survival and development. *Journal of Insect Science*, 11(1):96, 2011.

506 Kennedy, P. J., Ford, S. M., Poidatz, J., Thiéry, D., and Osborne, J. L. Searching for nests of the invasive Asian
507 hornet (*Vespa velutina*) using radio-telemetry. *Communications Biology*, 1(1):88, 2018.

508 Langkilde, T. and Alford, R. A. The tail wags the frog: harmonic radar transponders affect movement behavior in
509 *Icthyophaga lesueuri*. *Journal of Herpetology*, 36(4):711–715, 2002.

510 Le, Q. S., Kim, J., Kim, J., and Son, H. I. Report on work in progress of small insect tracking system using
511 autonomous uav. In *2017 14th International Conference on Ubiquitous Robots and Ambient Intelligence (URAI)*,
512 pages 242–243. IEEE, 2017.

513 Linander, N., Dacke, M., Baird, E., and de Ibarra, N. H. The role of spatial texture in visual control of bumblebee
514 learning flights. *Journal of Comparative Physiology A*, 204(8):737–745, 2018.

515 Lövei, G. L., Stringer, I. A., Devine, C. D., and Cartellieri, M. Harmonic radar—a method using inexpensive tags to
516 study invertebrate movement on land. *New Zealand Journal of Ecology*, pages 187–193, 1997.

517 Milanesio, D., Saccani, M., Maggiora, R., Laurino, D., and Porporato, M. Design of an harmonic radar for the
518 tracking of the asian yellow-legged hornet. *Ecology and evolution*, 6(7):2170–2178, 2016.

519 Mola, J. M. and Williams, N. M. A review of methods for the study of bumble bee movement. *Apidologie*, 50(4):
520 497–514, 2019.

521 Noutahi, E. Fisher’s exact test for mxn contingency table. 2018. doi: 10.5281/zenodo.2587757.

522 Nunes-Silva, P., Hilário, S. D., Santos Filho, P. d. S., and Imperatriz-Fonseca, V. L. Foraging activity in plebeia
523 remota, a stingless bees species, is influenced by the reproductive state of a colony. *Psyche*, 2010, 2010.

524 Nunes-Silva, P., Hrnčir, M., Guimarães, J., Arruda, H., Costa, L., Pessin, G., Siqueira, J., De Souza, P., and
525 Imperatriz-Fonseca, V. Applications of rfid technology on the study of bees. *Insectes sociaux*, 66(1):15–24, 2019.

526 O’Neal, M. E., Landis, D., Rothwell, E., Kempel, L., and Reinhard, D. Tracking insects with harmonic radar: a
527 case study. *American Entomologist*, 50(4):212–218, 2004.

528 Osborne, J., Williams, I., Carreck, N., Poppy, G., Riley, J., Smith, A., Reynolds, D., and Edwards, A. Harmonic
529 radar: a new technique for investigating bumblebee and honey bee foraging flight. In *VII International Symposium*
530 *on Pollination 437*, pages 159–164, 1996.

531 Osborne, J., Clark, S., Morris, R., Williams, I., Riley, J., Smith, A., Reynolds, D., and Edwards, A. A landscape-scale
532 study of bumble bee foraging range and constancy, using harmonic radar. *Journal of Applied Ecology*, 36(4):
533 519–533, 1999.

534 Osborne, J. L., Martin, A. P., Carreck, N. L., Swain, J. L., Knight, M. E., Goulson, D., Hale, R. J., and Sanderson,
535 R. A. Bumblebee flight distances in relation to the forage landscape. *Journal of animal ecology*, 77(2):406–415,
536 2008.

537 Philippides, A., de Ibarra, N. H., Riabinina, O., and Collett, T. S. Bumblebee calligraphy: the design and control of
538 flight motifs in the learning and return flights of *Bombus terrestris*. *Journal of Experimental Biology*, 216(6):
539 1093–1104, 2013.

540 Poissonnier, L.-A., Jackson, A. L., and Tanner, C. Cold and co₂ narcosis have long-lasting and dissimilar effects on
541 *Bombus terrestris*. *Insectes Sociaux*, 62(3):291–298, 2015.

542 Porporato, D. M. Life project number: Life14 nat/it/001128 final report. life stopvespa. Available
543 at[https://www.vespavelutina.eu/Portals/0/Users/152/52/152/Final%20Report%20LIFE14%20NAT%20IT%
544 20001128%20STOPVESPA%20-%20Abbreviated%20Version.pdf?ver=2020-04-17-184507-953\(2020/12/15\)](https://www.vespavelutina.eu/Portals/0/Users/152/52/152/Final%20Report%20LIFE14%20NAT%20IT%20001128%20STOPVESPA%20-%20Abbreviated%20Version.pdf?ver=2020-04-17-184507-953(2020/12/15)),
545 2019.

546 Psychoudakis, D., Moulder, W., Chen, C.-C., Zhu, H., and Volakis, J. L. A portable low-power harmonic radar
547 system and conformal tag for insect tracking. *IEEE Antennas and Wireless Propagation Letters*, 7:444–447, 2008.

548 Riley, J., Smith, A., Reynolds, D., Edwards, A., Osborne, J., Williams, I., Carreck, N., and Poppy, G. Tracking
549 bees with harmonic radar. *Nature*, 379(6560):29–30, 1996.

550 Riley, J. R. Adaption of harmonic radar for tracking tsetse flies. final technical report. Available at<https://assets.publishing.service.gov.uk/media/57a08dc0ed915d3cfd001bbe/R5457a.pdf>(2020/12/15), 1995.
551

552 Robert, T., Frasnelli, E., de Ibarra, N. H., and Collett, T. S. Variations on a theme: bumblebee learning flights
553 from the nest and from flowers. *Journal of Experimental Biology*, 221(4), 2018.

554 Roland, J., McKinnon, G., Backhouse, C., and Taylor, P. D. Even smaller radar tags on insects. *Nature*, 381(6578):
555 120–120, 1996.

556 Saville, N. M., Dramstad, W. E., Fry, G. L., and Corbet, S. A. Bumblebee movement in a fragmented agricultural
557 landscape. *Agriculture, Ecosystems & Environment*, 61(2-3):145–154, 1997.

558 Schaffer, M. J. *Spatial aspects of bumble bee (Bombus spp. Apidae) foraging in farm landscapes*. PhD thesis, Lincoln
559 University, 1997.

560 Shearwood, J., Hung, D., Palego, C., and Cross, P. Energy harvesting devices for honey bee health monitoring. In
561 *Advanced Materials and Processes for RF and THz Applications (IMWS-AMP), 2017 IEEE MTT-S International*
562 *Microwave Workshop Series on*, pages 1–3. IEEE, 2017.

563 Straw, A. D., Branson, K., Neumann, T. R., and Dickinson, M. H. Multi-camera real-time three-dimensional
564 tracking of multiple flying animals. *Journal of The Royal Society Interface*, 8(56):395–409, 2011.

565 Tahir, N. and Brooker, G. Recent developments and recommendations for improving harmonic radar tracking
566 systems. In *Proceedings of the 5th European Conference on Antennas and Propagation (EUCAP)*, pages 1531–1535.
567 IEEE, 2011.

568 Tasker, P., Reid, C., Young, A. D., Threlfall, C. G., and Latty, T. If you plant it, they will come: quantifying
569 attractiveness of exotic plants for winter-active flower visitors in community gardens. *Urban Ecosystems*, 23(2):
570 345–354, 2020.

571 Tsai, Z.-M., Jau, P.-H., Kuo, N.-C., Kao, J.-C., Lin, K.-Y., Chang, F.-R., Yang, E.-C., and Wang, H. A high-
572 range-accuracy and high-sensitivity harmonic radar using pulse pseudorandom code for bee searching. *IEEE*
573 *Transactions on Microwave Theory and Techniques*, 61(1):666–675, 2012.

574 Urbanowicz, C., Muñiz, P. A., and McArt, S. H. Honey bees and wild pollinators differ in their preference for and
575 use of introduced floral resources. *Ecology and Evolution*, 10(13):6741–6751, 2020.

576 Wilson, P. and Stine, M. Floral constancy in bumble bees: handling efficiency or perceptual conditioning? *Oecologia*,
577 106(4):493–499, 1996.

578 Wolf, S., McMahon, D. P., Lim, K. S., Pull, C. D., Clark, S. J., Paxton, R. J., and Osborne, J. L. So near and yet so
579 far: harmonic radar reveals reduced homing ability of nosema infected honeybees. *Plos one*, 9(8):e103989, 2014.

580 **Supplementary**

581 **Capture and Tagging**

582 A foraging bee is captured using a butterfly net (Watkins & Doncaster), placed in a marking cage (W & D), with a
583 mesh lid at both ends, and placed in either a freezer or ice box (containing ice and salt) to induce narcosis to enable
584 tagging to take place. A small 12V 8cm computer fan, powered with a 9V battery, is used to ventilate the marking
585 cage, which we found helps reduce the bee's temperature quickly. Although a widely used approach, we note that
586 issues do exist with immobilising bees using cold (or CO₂) (Poissonnier et al., 2015). We were also able to attach a
587 tag without cold or CO₂ using a standard queen marking tube with plunger for the *Bombus terrestris* in Section
588 3.2.1. However, the tube mesh limits us to very small tags and we found it more likely to result in failed tagging.

589 **Hardware Notes**

590 To aid replication we elaborate below on several aspects of the hardware design that we found were necessary for
591 successful operation.

592 **Choice of camera** Initial versions of the system used a consumer compact camera (PowerShot SX210, Canon) in
593 which access to the SD card was controlled by connecting or disconnecting the USB power lines from a raspberry pi.
594 Triggering was via a mechanical actuator and flash control was via decoupling the connected slave-triggered flash.
595 We more recently have been using the MV-CA032-10GM (HIKROBOT) camera successfully (2048 × 1536).

596 **Flash and power** The TT560 has a 35mm full power guide number of 38m although was used at 1/16 power.
597 Several other low-cost flashes were also used successfully (including the YN560-II, Yongnuo). The choice of 1/16
598 was determined empirically while also optimising the exposure duration. It was the point at which a reduced signal
599 to background became apparent. We found somewhat variable brightness in the images however, suggesting either
600 the flash power or the timing of the flash or camera trigger can vary slightly.

601 **EMP protection** Each flash (and its trigger cable) was wrapped in aluminium thermal insulation tape and then
602 electrically insulated with a layer of duct tape. Without this the electromagnetic pulse from the flash-bulb caused
603 the other flashes to also trigger. This didn't matter when using the flashes in a combined approach but was necessary
604 for sequential triggering.

605 **Filter** Earlier in the project we used a near-UV colour glass filter (50x50mm, 390nm Band-pass, Knight Optical)
606 based on the observation that most light impinging our camera will be from foliage which reflects little light at the
607 blue/violet end of the visible spectrum. However we found that most false positives and noise were caused by other
608 non-foliage objects so this filtering didn't help and also caused an inevitable reduction in signal strength.

609 **Platform** For the experiments in this paper we used a simple stepladder or a convenient building to provide
610 elevation. Previously we have explored the use of a 10m guyed mast (portable folding aluminium telescopic mast,
611 damsu.co.uk), a tethered helium balloon (giant cloudburst chloroprene balloon, balloons.co.uk) and a multicopter

612 UAV. The UAV may have future impact as a method for continuously following the target but has a very limited
613 battery life. The balloon can remain in place longer but can only be used in very calm conditions. The mast is
614 shorter and less flexible but provides stable images allowing more accurate tracking. We would suggest a 2m or 3m
615 photography light stand as an ideal platform in future providing a good compromise.

616 **Costs** A brief note on costs, to emphasise the relative low-cost nature of the system, overall it cost about £660. The
617 electronic-shutter camera itself was the most expensive component at £470. All other items came to about £190.
618 We are experimenting now with a lower resolution camera (MV-CE013-50GM, HIKROBOT, 1280×960) which costs
619 £205. If this works the unit cost would be about £400. The retroreflectors and glue are almost free ($<£0.02/\text{bee}$).

620 **Software Notes**

621 **Other components** The implementation of the detection algorithm also checks for broken or skipped frames and,
622 by comparing average brightness it checks whether the flash has fired (or has failed, e.g. due to a low flash battery,
623 and warns the user). It also looks for large movements (e.g. if the camera is moved) and avoids using images from
624 before the movement in the algorithm above. Finally, in step 4 above, rather than compare with all previous images
625 we typically just use images from the last 9 photo-pairs, to save time and memory.

626 **Deployment** Two python modules have been written to collect and analyse the camera images in real-time
627 on-board the tracking system. The full code is available to download and use from github.⁷ Besides the detection
628 described above, the software also controls the flashes and camera, saves the data to the SD card and can control
629 a servo if mounted on a rotating platform. Finally it provides a web (and API) interface to the system, allowing
630 field workers to control many aspects of the system (either from a smartphone or laptop). These include the flash
631 configuration and frequency, the detection threshold, etc. The interface also displays the current (and previous)
632 images and targets found (if any) and produces an audio alert on detecting a retroreflector. The system either
633 provides a hotspot or uses a local hotspot (e.g. generated by a smartphone). Other services include high-precision
634 ($<1\text{ms}$ error) synchronisation of the datetime onboard using the phone or laptop's clock, so multiple systems used in
635 3D flight path reconstruction can have accurate timestamps on their images.

636 **The maximum-dilate operation, $D_M(\cdot)$**

637 In the algorithm with use the maximum-dilate operation on either non-flash photos $NF_i^{(j)}$ or on previous subtraction
638 results B_n . The reason is that in both a non-target bright object may have moved a small amount between the two
639 images being subtracted, either due to image misalignment or due to physically moving, e.g. a flower moving in the
640 wind. We still need to ensure this object is 'cancelled' when the one image is subtracted from another. Ideally then
641 we wish to use for subtraction an image (generated by the $D_M(\cdot)$ function) in which each pixel is the maximum

⁷https://github.com/lionfish0/bee_track and <https://github.com/lionfish0/retrodetect>.

642 value of all pixels within a certain distance w . Specifically, if $A = D_M(B)$ then,

$$[A]_p = \max_{q, |q-p|_2 \leq w} [B]_q. \quad (1)$$

643 Computing this exactly takes a few seconds on the raspberry pi. So for efficiency we compute an approximation.
644 First the image is downscaled by 10 in each direction, but each pixel in the new image is the maximum of the
645 10×10 grid of original pixels. We then perform the exact calculation, in (1), on this reduced image, before scaling
646 back. This gives a slightly pixelated result to the image being subtracted, but is sufficiently accurate for the system
647 to function.

648 Effect of Tags

649 An important question when applying novel tags or labels to animals for tracking is to determine what effect the
650 tags have on behaviour and survival.

651 Our tags weigh approximately 5mg, which is at the smaller end of the passive radio tag range - Osborne et al.
652 (1999) used harmonic radar tags weighing 12 mg. Other attempts vary between 1 - 20mg (Daniel Kissling et al.,
653 2014). Importantly though our tags don't require an aerial. In Osborne et al. (1999) the aerial extends 16mm and
654 some concern is expressed about the effect of the aerial on behaviour. The 5mg tag compares favourably to the
655 weight of *B. terrestris* workers at 68 to 754 mg (Goulson et al., 2002). Smaller tags were used with *Apis mellifera*
656 workers which are considerably smaller, between 51 and 209 mg (Kaftanoglu et al., 2011) so the tag was still less
657 than 10% of the insect's weight.

658 Anecdotally, we noted that, immediately after tagging, the bees would often spend a few minutes grooming.
659 Later, all the re-observed insects appeared to return to 'normal' behaviour and would be seen foraging.

660 The most serious issue with the tags was associated with the artificial nests of *B. terrestris* colonies (Biobest,
661 standard hive). The ridge on the tags would very frequently become entangled in the cotton-wool provided within
662 the hive for thermal insulation. We found the non-cotton-wool nest performed better (although may only be suitable
663 for the warmest parts of the year). One might also consider reducing or avoiding the ridge but this will reduce the
664 signal and range of the system. Conversely we saw several tagged *wild* bees foraging a week after tagging, suggesting
665 that wild bees did not have such issues in their own nests (which don't contain cotton wool).

666 For a more quantitative assessment of tag effect we followed a similar approach to Hagen et al. (2011), comparing
667 the time spent foraging of tagged and untagged bees. Our experiment was rather less powerful however, as we
668 just looked at foraging time on the flower patch (which probably varies more, especially as we looked at multiple
669 flower types) and we only recorded from when the bee is first seen. In detail: An observer arrives near the forage
670 patch, selects a bee and records the time the bee remains foraging before leaving the flower patch (recording also the
671 species and caste of bee, plant and whether the bee has a tag). This introduces (unbiased) additional noise to the

672 data, as the length of the entire foraging session was not recorded. The observer preferentially selected tagged bees,
673 to ensure a roughly balanced dataset. Overall 21 tagged and 19 untagged bees were recorded (respectively 9 and
674 6 of these were *B. terrestris*, 7 and 2 of these were *B. lapidarius*, other species had fewer samples). Considerable
675 variation in foraging times was present (with times recorded between 6 and 509 seconds). The samples were recorded
676 at two field sites. To further increase the number of samples we would suggest more field sites should be included so
677 that the same bees were not being repeatedly sampled (which could artificially inflate significance, for example if
678 one individual happened to be very slow or fast).

679 Hagen et al. (2011, figure 2b) found a significant, 4 fold increase in foraging time for the tagged bees. We did
680 not find any significant difference between the two groups (using mann whitney U or a t-test on the log-times)
681 either within species (e.g. *B. terrestris*: $r = 21$ [$p = 0.52$] $t = 0.75$ [$p = 0.46$], *B. lapidarius*: $r = 4$ [$p = 0.46$] t
682 $= 1.11$ [$p = 0.30$]) or pooled ($r = 146$ [$p = 0.15$] $t = 1.58$ [$p = 0.12$]). Exponentiating the 95% confidence interval
683 for the difference in log times Tagged/Untagged pooled: [0.85 - 3.66], which compares favourably to tags used in
684 Hagen et al. (2011), although our sample size is small. We also split the data by flower species, and considered both
685 separate species and pooled, but found no significant differences between the tagged and untagged bees, in any of
686 these tests (no correction was made for these multiple comparisons).

687 **Theoretical Range and Signal**

688 The actual range over which this system could work is difficult to compute as the main source of noise the background
689 landscape and ambient light. One can potentially estimate the relative effectiveness with respect to distance. The
690 apparent size of the reflector will fall by the square of the distance. The light it receives from the flash will also fall
691 by the same. Hence the signal from the reflector will fall proportional to $1/d^4$. Thus if one doubled the camera flash
692 brightness, one would only achieve a 19% increase in range. This relationship is part of the *radar equation*.

693 We briefly set out a rough sketch of the physics behind the process, to help explain why the reflector is visible.
694 We consider the theoretical potential of the system by considering the proportion of the reflected light that is from
695 the flash compared to the energy from the general background. We do not consider the issue of specular reflections
696 which may result in brighter points than the diffuse light one would normally see in a natural environment. A
697 typical speedlight, taking into account inefficiencies, will release about 2.5J of visible light energy at 1/16 power
698 over $50\mu\text{s}$. We assume approximately the area illuminated by our flash is equal to the distance from the system
699 squared, so if the system is 30 metres from the target the flash will provide 56Wm^{-2} . At its brightest, sunlight can
700 transmit 445Wm^{-2} of *visible* light to the Earth's surface. If we use a 3 Megapixel camera covering the same area
701 as the flash, one pixel (from 30 metres) is $3 \times 10^{-4}\text{m}^2$. We assume the sunlight and flash light will be reflected
702 from the landscape in a diffuse manner, with an albedo of e.g. 0.3, so at the distance of the camera, assuming
703 the light is reflected in all directions equally, the reflection from the background from each pixel will provide a
704 power density of $0.3 \times (3 \times 10^{-4}) \times (445 + 55)/2\pi 30^2 = 8.0\mu\text{Wm}^{-2}$ for that pixel. A 10mm^2 retroreflector 30m

705 away will be illuminated by the flash with $556\mu\text{W}$. Hawkins et al. (2003) suggest that for a good retroreflector
 706 about half the reflected energy is reflected within 0.3 degrees of the entrance angle, which at 30m will cover an
 707 expanse of only 0.1m^2 . So will have a power density of $2814\mu\text{Wm}^{-2}$. Thus the pixel with the retroreflector in will
 708 return hundreds of times more power. It is important to stress that *specular* reflection from litter, metal objects or
 709 water can overwhelm this ratio, leading to false positives in the image. Hence the additional processing steps we
 710 conduct to remove these artifacts. These calculations show how, in principle, the small reflector can be detected
 711 from a considerable distance. The exposure typically won't align correctly with the flash increasing substantially
 712 the influence of sunlight, the retroreflector is often at an angle further reducing the signal. We next evaluate the tag
 713 empirically to confirm what range is practically possible.

714 **List of Authorities**

| | |
|--|-----------------|
| <i>Apis mellifera</i> | Linnaeus, 1758 |
| <i>Megachile</i> sp. | Latreille, 1802 |
| <i>Bombus lapidarius</i> | Linnaeus, 1758 |
| 715 <i>Bombus terrestris</i> | Linnaeus, 1758 |
| <i>Bombus terrestris</i> subsp. <i>audax</i> | Harris, 1776 |
| <i>Bombus</i> spp. | Latreille, 1802 |
| <i>Bombus hortorum</i> | Linnaeus, 1761 |